Learn to pay attention: distinct development of activity in dorsal and ventral medial prefrontal cortex

V.P.M. Borges[1*]

[1]Laboratory of Integrative Neurophysiology (INF), Center for Neurogenomics and Cognitive Research (CNCR), Vrije Universiteit Amsterdam, Netherlands

*** Correspondence:**
Vinicius Borges

mecanismoseducacao@gmail.com

Keywords: attention, learning, prefrontal cortex, fiber photometry, 5CSRTT

Abstract

The dorsal medial and ventral medial prefrontal cortices (dmPFC and vmPFC) are involved in executive function processes such as working memory, inhibitory control, and decision making. The functions of these two regions have been extensively studied with the 5-choice serial-reaction time task (5CSRTT) for many decades, however, all of the current literature has investigated what happens after the animal has already learned the 5CSRTT: there is no current knowledge on what happens in the brain of a rat during the learning stages of the 5CSRTT. Therefore, the aim of this study was to characterize the training-induced development of neuronal activity of dmPFC and vmPFC in the rat brain during the learning stages of the 5CSRTT using fiber photometry. We found that the dmPFC becomes more active in later stages of learning while the vmPFC becomes less active in later stages of the 5CSRTT. This difference reflects the different connections of these brain regions and it may be caused by the development of different cognitive processes: the dmPFC is involved in motor coordination and task accuracy, and it becomes more active as the task becomes more difficult; whilst the vmPFC is involved in integration of sensory input and impulsivity, and it becomes less active as the task becomes more habitual.

1 Introduction

The prefrontal cortex (PFC), defined as the rostral-most section of the frontal cortex, is involved in cognitive processes such as working memory, inhibitory control, and decision making, which are collectively known as ‘executive functions’ (Domenech & Koechlin, 2015). The PFC can be considered ‘the goal-oriented cortex’ (Carlén, 2017) because it integrates information from the basal ganglia, subcortical and neocortical structures in order to orchestrate adaptive behavior (Kesner & Churchwell, 2011). In the rat, the PFC is divided into three main anatomical regions: ventral, lateral and medial (Heidbreder & Groenewegen, 2003). The medial PFC can be further subdivided into ventral (vmPFC) and dorsal (dmPFC) subregions. The dmPFC constitutes the precentral (PC) and anterior cingulate (AC) cortices while the vmPFC constitutes infralimbic (IL), medial orbital (MO) cortices (Uylings & Van Eden, 1991). The prelimbic (PL) cortex is thought to be part of both dmPFC and vmPFC, with no clear anatomical division between them, but rather a gradient of neuronal projections to basal and subcortical structures (Gabbott et al, 2005). (**Figure 1**)

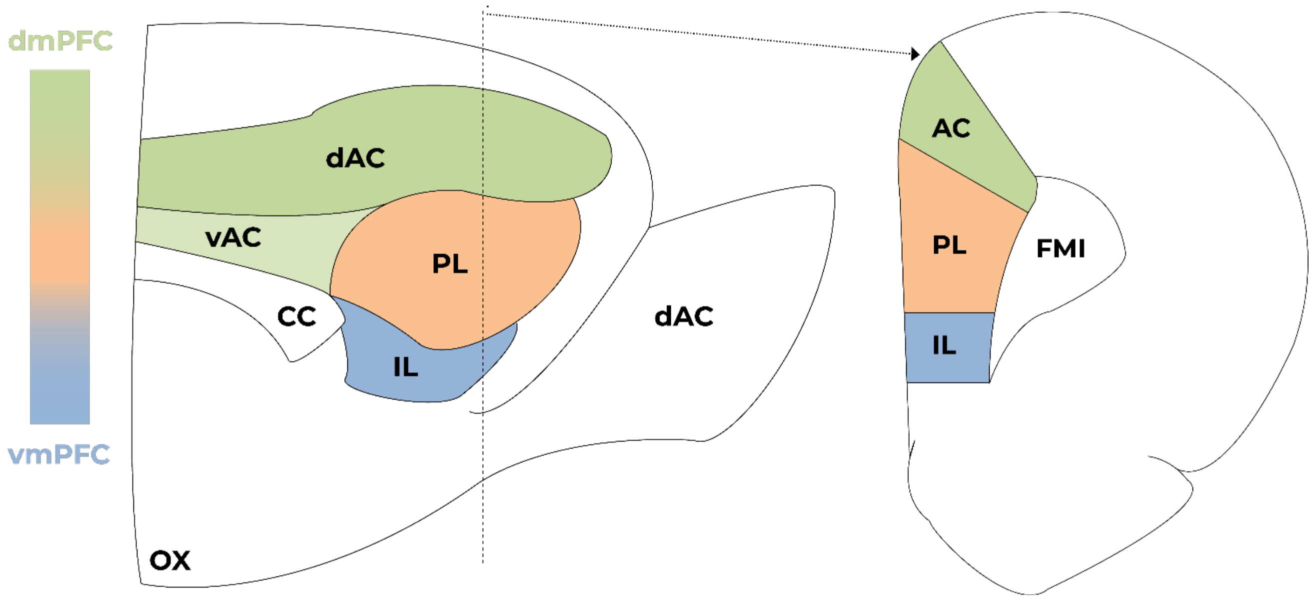

Figure 1. Coronal section of the rat's prefrontal cortex. Adapted from McKleven (2015).

One of the most well-established paradigm to assess executive functions is the 5-choice serial-reaction time task (5CSRTT) (Robbins, 2002), which has been used for decades because of the relative ease of training animals and the great reliability of within-subject performance (Higgins & Silenieks, 2017). In this task, the rats are placed in an operant chamber and are then required to scan a horizontal array of five holes which are pseudorandomly illuminated 5 seconds after the animal initiates a trial. If the animal performs a nose poke in a timely manner, it is rewarded with a food pellet. As the animal progresses through the learning stages, the time that the cue light is on, called the 'stimulus duration (SD)', is reduced in order to escalate the difficulty of the attentional task. During the learning stages of the 5CSRTT, the animal not only must learn the contingency of 'poking the right hole to get a reward', but it must also desire the outcome and therefore perform the task correctly to achieve it — in other words, the animal needs to establish and pursue a goal (Dalley, Cardinal, & Robbins, 2004). Within the 5CSRTT paradigm, the functions of different mPFC subdivisions have been studied for many decades using a variety of interventions, such as lesion studies, electrophysiology and more recently chemogenetics, optogenetics and fiber photometry (**Table 1**).

Table 1. Summary of current 5CSRTT literature on the mPFC, dmPFC and vmPFC.

Intervention type	mPFC	dmPFC	vmPFC
Lesion studies	Lesion decreases accuracy and increases preservative responses [a]	Lesion impairs accuracy, but has no effect on impulsivity [b] Lesion increases omissions [c] ACC lesion decreases accuracy and increases omissions [d]	Lesion decreases accuracy briefly and increases preservative responses [b] Lesion decreases accuracy [c] IL lesion decreases response latency; increases omissions and preservative responses [d]
Electrophysiology	mPFC is active during the entire prepatory phase [e] Gamma oscillations relate to cue presentation and correct responses, theta oscillations relate to the waiting period and response outcome [f] Premature responses incur in neuronal ramping activity earlier than correct responses [g] FS-PV neurons increase activity after trial start, but activity is only sustained in correct trials [h]	dACC is active during anticipation of visual cues - involved in error-related events and preparatory attention [e] ACC drives claustrum microcircuitry, which in turn fires at the 1-to-10 hz frequency and closely relates to 5CSRTT performance [i]	-
Chemogenetics	Activation of cholinergic neurons increases attention; but overactivation leads to decreased accuracy [j] Inhibition of PFC-projecting dopaminergic neurons decreases attention, but not impulsivity [o]	Inactivation of dACC increases omission/ response delay and decreased accuracy [k]	-
Optogenetics	Inhibition of FS-PV neurons decreases accuracy; Excitation of FS-PV increases accuracy [h] Activation of PFC projecting serotonergic neurons decreases impulsive responses; inactivation increases impulsivity [n]	Inhibition during the entire preparatory stage disrupts accurracy [l] Silencing ACC neurons projecting to claustrum decreases accuracy [m]	Inhibition two seconds before cue presentation disrupts accuracy; inhbition during the entire preparatory stage increases accuracy [l]
Fiber Photometry	PFC-projecting serotonergic neurons increase activity during the waiting period and upon reward consumption [n]	Activity of ACC afferents to claustrum was increased prior to cue presentation in correct trials, not incorrect ones [i]	-

a. Muir et al. (1996) b. Passetti et al. (2002) c. Maddux & Holland (2011) d. Chudasama et al. (2003) e. Totah et al (2009) f. Donnelly et al. (2014) g. Donnelly et al. (2015) h. Kim et al. (2016) i. White et al. (2018) j. Fisher (2018) k. Koike et al (2016) l. Luchicchi et al. (2016) m. Panicker (2016) n. Wang (2017) o. Boekhoudt et al. (2016)

Lesion studies have been used for many decades because of the relative simplicity of the surgical process. The underlying premise of this type of study is that ablations of certain brain regions are related to subsequent changes in behavior. Muir, Everitt, & Robbins (1996) found that an overall ablation of the mPFC leads to a decrease in accuracy and increase in preservative responses, demonstrating that the mPFC mediates some aspect of attentional selectivity and behavior flexibility. A few years later, the same group demonstrated the functional distinction of mPFC regions: damaging the dmPFC impairs accuracy but does not change impulsive responses, while damaging the vmPFC decreases accuracy and increases preservative responses (Passetti, Chudasama, & Robbins, 2002). Maddux & Holland (2011) found a different result: vmPFC ablation leads to an increase in incorrect responses, while dmPFC ablation increases omissions. Chudasama et al. (2003) specifically showed that IL lesioning induces premature responses, OFC lesioning leads to preservative responses and ACg lesioning leads to deficits in attentional selectivity. Although lesion studies were commonplace for decades, they are strongly limited by within-subject irreversibility and non-specificity, since lesion agents such as quinolinic acid degenerate excitatory and inhibitory neurons, as well as both cell bodies and axons. Furthermore, ablation of certain brain regions may induce compensatory mechanisms, such as overactivation of connected areas, which could potentially be the cause of a change in behavior instead of the damaged region itself (Fuster, 2015).

Electrophysiology studies also have been a standard in behavioral research for decades, mainly due to their great temporal resolutions. Totah et al. (2009) used electrophysiology to show that the dACC is active during the anticipation of visual cues and when error-related events occur, while the mPFC is active during the preparatory period only. Donnelly et al. (2014) discovered that, in the mPFC, gamma oscillations are related to cue presentation and correct responses, while theta oscillations are related to the waiting period and response outcome. The same group later showed that: (1) neurons in the mPFC signal the trial outcome only after an action was performed; (2) there is a ramping activity in mPFC neurons during both correct and premature trials, however premature responses incur in ramping activity earlier than correct responses (Donnelly et al 2015). Kim et al. (2016) demonstrated that fast-spiking parvalbumin neurons increase activity after trial start, but activity is only sustained in correct trials. Elaborating on this finding, White et al. (2018) demonstrated that ACC drives claustrum microcircuitry with both parvalbumin positive and negative interneurons; claustrum activity in the 1-to-10 hz frequency closely relates to ACC activity during the 5CSRTT. The main disadvantage of electrophysiology compared to other techniques is their non-specificity in distinguishing different neuronal populations. (Carter & Shieh, 2015)

In the past decade, chemogenetics and optogenetics became a new gold-standard of behavioral research. Both techniques have strong advantages over other interventions: the expression of DREADDs or light sensitive receptors can be very specific to a subpopulation of neurons, both techniques provide within-subject reversibility and great spatial resolution (Carr, de Vries, & Pattij, 2018). However, these techniques also have disadvantages: the uneven expression of receptors due to a limitation of efficiency in transfection and the unknown effect of the activating mechanisms (either CNO or light) in the brain (Campbell & Marchant, 2018; Frank et al., 2016). Using chemogenetics, Koike et al. (2015) showed that inactivation of the dACC during 5CSRTT leads to an increased number of omissions and greater response delay and a decrease in accuracy. Boekhoudt et al. (2016) showed that activation of PFC-projecting dopaminergic neurons leads a decrease in accuracy, but has no effect on impulsivity. Fisher (2018) showed that both activating cholinergic neurons in the mPFC increases attention, but overactivating the same neurons leads to a decrease in performance. Using optogenetics, Luchicchi et al. (2016) demonstrated that optogenetic inhibition of vmPFC for two seconds before cue presentation stage was enough to disrupt accuracy, while the dmPFC needed to be inhibited during the entire preparatory stage to hamper performance - interestingly, inhibition of the vmPFC for the entire preparatory stage resulted in an increase in accuracy. Panicker (2016) found that silencing claustrum-projecting ACC neurons lead to a decrease in attentional performance. Kim et al. (2016) found that silencing fast-spiking parvalbumin neurons in the mPFC lead to decreased performance in the 3-CSRTT, and enhancing this neuronal subpopulation caused an increase of task accuracy, indicating that FS-PV neurons are related to goal-driven attention processing.

In summary, the rat vmPFC and dmPFC have distinct anatomical connections and mediate different cognitive functions: the vmPFC has seems to be involved in attentional and response selection functions, which has been extensively demonstrated using paradigms other than the 5CSRTT (De Bruin et al., 1994; Ragozzino, Wilcox, Raso, & Kesner, 1999) - in particular, the infralimbic and prelimbic cortices seem to have opposing functions in directing proactive behavior (Hardung et al., 2017). On the other hand, the dmPFC seems to mediate the coordination of action and motor sequencing behaviors (Otani, 2004), and the AC in particular seems to be highly active when cognitive conflicts arise. (De Wit et al., 2006; Seamans, Lapish, & Durstewitz, 2008)

Although there are many studies that have analyzed the mPFC after the rat has learned the 5CSRTT, there is no literature on the changes of this brain region during the process of learning the paradigm. This constitutes a significant knowledge gap because it is known from previous studies, using different paradigms other than the 5CSRTT, that the PFC is more active during learning stages of an activity and it becomes less active when the actions to perform the task become habitual, as evidenced by electrophysiology (Barnes et al., 2005), pharmacological (Coutureau & Killcross, 2003) and fiber photometry (Kupferschmidt et al., 2017) studies. This lack of knowledge can in part be attributed to limitations in technology: methods to analyse neuronal activity in vivo, in real-time and in freely moving animals – such as fiber photometry and the miniscope – were made viable only in the past decade (Girven & Sparta, 2017).

Fiber photometry, the technique of choice for this study, is a technique that optically records calcium ion transient activity, which serves as a well-established proxy for neuronal activity (Chen et al., 2013). Even though FP lacks cellular resolution, it is a great technique to analyze synchronous activity dynamics within a specific brain circuit (Resendez & Stuber, 2015). Wang (2017) used the technique to demonstrate that PFC-projecting serotonergic neurons increase activity during the waiting period and upon reward consumption in the 5CSRTT. In the context of 5CSRTT, White et al. (2018) used FP to demonstrate that the activity of claustrum-projecting ACC neurons increases before cue presentation in correct trials, but not incorrect trials.

The aim of this study was to investigate what are the changes in patterns of neuronal activation in the dmPFC and vmPFC in the rat brain during the learning acquisition stages of the 5CSRTT. We expected to observe: (1) A difference in patterns in dmPFC and vmPFC due to their different connections to other brain regions; (2) A change in the signal as the rats advance though the learning stages and the task difficulty increases and (3) A decrease in calcium transient activity in both vmPFC and dmPFC once the rats have mastered the task, since habits require less cognitive processing than the learning stages of goal-directed actions (Smith et al., 2014).

2 Materials and Methods

Animals

11 Male Long Evan rats (Janvier Labs, France; 10 weeks old at the start of the experiments) were used in this study. The Long-Evans strain was chosen because these rats learn cognitive tasks faster than both Sprague-Dawley (Turner & Burne, 2014) and Wistar (Ambrogi Lorenzini, Bucherelli, Giachetti, & Tassoni, 1987) strains – although they are more aggressive and difficult to

handle. All animals were housed individually, in an environment with controlled temperature (21 ± 2 °C) and humidity (50-55%) on 12-hour light/dark reversed cycle (lights OFF: 7 AM). Animals were individually housed and put on food restriction one week before the learning task while maintaining 85-90% of the free-feeding body weight in order to increase motivation of the learning task. Water was given ad libitum.

The animal ethical care committee of the VU University and VU University Medical Center approved all experimental procedures, which were in accordance with European and Dutch law.

Stereotaxic surgery

Before surgery, the animal was anesthetized with isoflurane (5%), placed on a heated pad and head-restricted using a stereotaxic device in a flat skull position. Body temperature was kept at 36.5 degrees. Anesthesia was applied before the start of the surgery (systemic: buprenorphine 0.05 mg/kg and carprofen 5mg/kg subcutaneous injections; and local: lidocaine subcutaneous injections). The head was shaved, disinfected with iodopovidone and the scalp skin was retracted. One 1-mm hole was drilled above the mPFC. In the dmPFC group, virus injections were done under a 10 degree angle at AP +2.76mm; ML ±1.49 mm; DV −2.94 and −2.84 mm relative to bregma; in the vmPFC group, they were made at AP +2.76 mm; ML ±0.5 mm; DV −4.65 mm from bregma. Viruses pAAV5-hSyn1-GCaMP6m ~2.4 x 10^{12} Gml^{-1}(UPenn Vector Core) were infused at 138 nl/min using a Nanoject II and a glass injection pipette (Drummond Scientific). Three guide screws were attached to the skull, and a chronic fiber optic cannula (Doric) with a diameter of 400 µm and 0.48 numerical aperture was inserted in the rat brain. The fiber optic cannula was implanted via the same hole as the viral injection and it was fixed to the skull using UV-cured dental cement (RelyX, 3M). After surgery, rats stayed on the same heated pad until ambulatory and were then individually housed in their home cage.

5-choice serial-reaction time task (5CSRTT)

Before each session, the sleeve on top of the animal's heads was cleaned with ethanol 70%. The rats were then placed in a standard 5-hole operant chamber (MedAssociates, Fairfax, Vermont USA), which were located inside of a sound-attenuating and ventilated cubicle to minimize distracting noises and smells from the room. The optic fiber was attached to a patch cable that included a fiber photometry-optimized rotary joint (FRJ_1x1_FC-FC, Doric), the fiber was attached to the rats' head using plastic mating sleeves (ADAF1 and ADAF2, Thorlabs). During the trials, the animals received 45 mg food reward pellets (Dustless Precision pellets, BioServ), which are more palatable than their normal chow diet (Envigo Teklad 2016). The operant chamber interfaced with custom hardware and behavioral data was captured by the Software Med Associates IV.

In the 5CSRTT, there are 4 possible types of responses: correct, incorrect, premature and omissions (**Figure 2**). Correct responses are characterized by a timely nose poke in the illuminated hole (a window of 3s starting at the moment of cue presentation), while incorrect responses occur when rats perform a nose poke in the incorrect hole (one of the four holes that were not illuminated). Incorrect responses are followed by a time-out period, in which the house light fully illuminates the cage for 5 seconds as a mechanism of negative reinforcement (Barker et al., 2010). The performance accuracy is defined by the ratio between correct divided by correct + incorrect responses. Omissions occur when the animal starts a trial and does not perform a nose poke in one of the apertures in a timely manner, which are also followed by a time-out period. Premature responses happen when the rat starts a trial, but it performs a nose poke before any of the holes were illuminated, and it also incurs in a time-out.

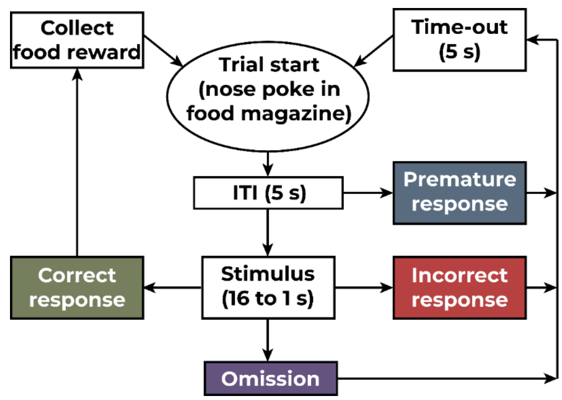

Figure 2. Flowchart of possible responses in the 5CSRTT. Adapted from Bari, Dalley & Robbins (2008).

This study used a 5CSRTT learning paradigm with 9 stages (**Table 2**). In stage 1, the animals received pellet rewards immediately after a nose poke, to ensure that they associate the food reward with the magazine location. In stage 2, all five holes are illuminated and a nose poke in any of them is rewarded, which creates the contingency between nose poking in the apertures and the food reward. In stage 3, only one hole is illuminated, and an incorrect nose poke incurs in a time-out period. In these first three stages, there are no omissions or premature responses. In all subsequent stages, each trial has a defined stimulus duration after the trial start and the stimulus duration became increasingly shorter. Rats progressed through the next stage after they have done more than 50 trials with an accuracy greater than 80% and less than 40% of omissions – this threshold of omissions was previously established by Luchicchi et al. (2016), it is significantly higher than most literature – 40% against 20% – since the animals have their performance hampered by the cable attached to their heads.

Table 2. Definition of learning stages and progression criteria of the 5-choice serial-reaction time task.

Level	Session (min)	Reward Duration (s)	Time Out (s)	SD (s)	ITI (s)	Progression criteria
1	30	5	-	-	-	Magazine training (over 50 trials)
2	30	5	5	∞	5	Over 50 trials
3	30	5	5	∞	5	Over 50 trials
4	30	5	5	16	5	>50 trials >80% accuracy <40% omission
5	30	5	5	8	5	>50 trials >80% accuracy <40% omission
6	30	5	5	4	5	>50 trials >80% accuracy <40% omission
7	30	5	5	2	5	>50 trials >80% accuracy <40% omission
8	30	5	5	1.5	5	>50 trials >80% accuracy <40% omission
9	30	5	5	1	5	>50 trials >80% accuracy <40% omission
vITI	60	5	5	1	5/7.5/15	Animal must complete 7 sessions
vSD	60	5	5	1/0.5/0.2	5	Animal must complete 3 sessions

Fiber photometry

Fiber photometry (FP) is a method which uses a single optical fiber to excite genetically encoded reporters and transmit the excitation light back along the same cable to a photodetector. In this study, we used a calcium indicator, GCaMP6, which is a recombinant protein formed from the fusion between GFP, calmodulin and M13. It was first developed in 2001 (Nakai, 2001) and several generations of the protein have been developed over the last two decades, improving pharmacological parameters and signal to noise ratio. In this study, we used the sixth generation of GCaMP – GCaMP6 – which was developed using high-throughput mutagenesis screening (Chen et al., 2013). We chose to use GCaMP6m because it strikes a good balance between detection efficiency and fast kinetics.

When a neuron is active, there is more calcium available in all cell compartments, including soma, dendrites, axons (Ross, 1989). Calcium plays an important role in many neurobiological functions, including exocytosis of neurotransmitters (Augustine, Charlton, & Smith, 1985) and synaptic plasticity (Zucker, 1999). When the ion binds to GCaMP6, the molecule changes its conformation allowing calmodulin and M13 to interact, causing the chromophore to increase the intensity of fluorescence (**Figure 3**). This difference in fluorescence can be detected in real-time and in freely moving rats using fiber photometry.

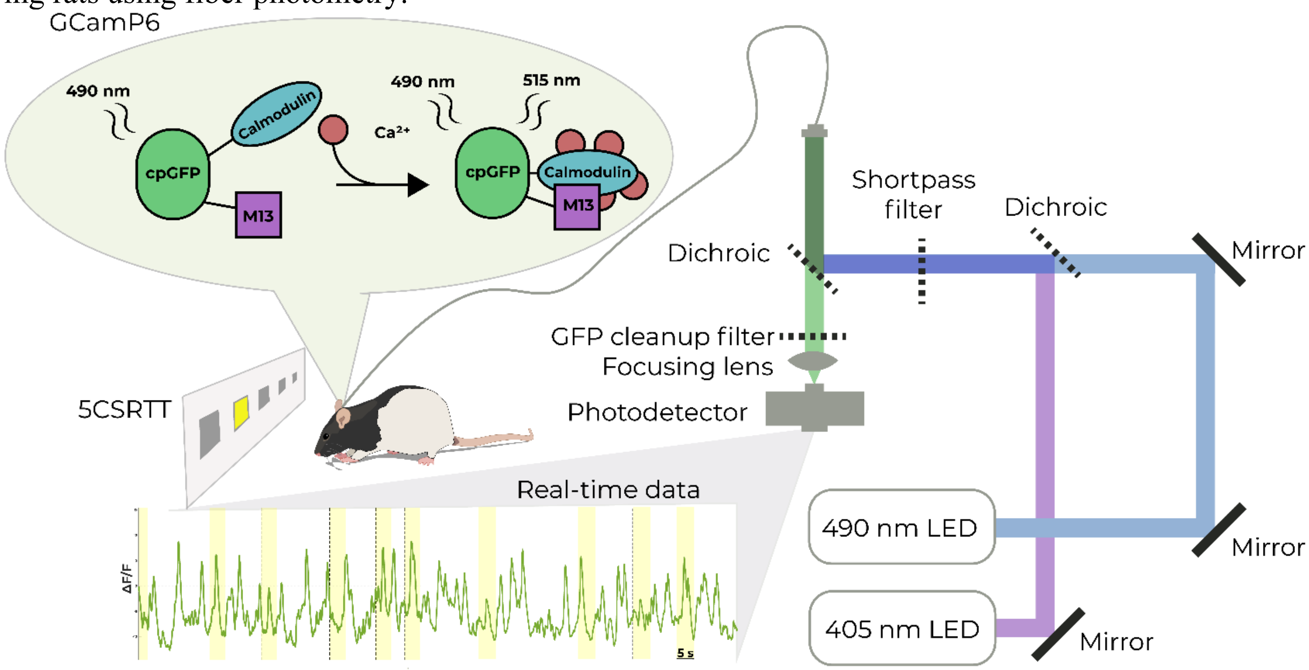

Figure 3. The photometry setup used in the study. Adapted from Zalocusky et al. (2016) and Girven & Sparta (2017).

The FP system used in this study was purchased as part of the Synapse package (Tucker Davis) and it is based on the setup described in (Zalocusky et al., 2016), a advancement on the original setup described in (Gunaydin et al., 2014) – it uses LEDs instead of lasers for the excitation of GCaMP and it contains a 405 nm LED (violet) in addition to the 490 nm (blue) channel (Thor Labs M490F1 and M405F1). The single fiber patch cord (MFP_400/440/LWMJ-0.53_#.#_FC-ZF2.5, Doric) serves for both excitation of and collection of emitted fluorescence. The blue light excites the GFP portion of GCaMP6m, while the violet light does not excite GFP and serves as an isosbestic/control channel, allowing for the correction of bleaching, movement artefacts and removal of other fluorescent molecules in the neuron, such as flavoproteins.

The blue and violet LEDs were modulated at 211 Hz and 531 Hz, respectively, before being passed through a 405 nm filter Doric (FMC4_AE(405)_E(460-490)_F(500-550)_S) which avoided contamination from ambient light (120 hz and harmonics). This separation of frequencies allows for the demodulation of the signal into two components: one that contains GCaMP6 fluorescence and one that contains background fluorescence. Both emitted signals were combined by a 425 nm dichroic mirror (Doric (same filter set as above)) and transmitted to the rat brain via a 400 µm 0.53 NA patch cord (Doric, Quebec, QC, Canada).

Fluorescence signals were collected by a photoreceiver (Newport Femtowatt, 2151). The signal interfaced with the lock-in amplifier RZ5P (Tucker Davis Technologies) – which is sensitive in the scale of nanovolts – and it was recorded by the software Synapse (Tucker Davis Technologies). Behavioral responses in the operant chamber were relayed to the RZ5P using a MedAssociates SuperPort (DIG-726, MedAssociates) and corresponding cable (CMF, Tucker Davis Technologies). Using this system, we were able to reliable record our rats for more than three months.

Histological verification

Transcardial perfusions are done to fixate soft tissues and are often done with aldehyde-based chemicals – in this case, paraformaldehyde (PFA). After a lethal injection of Euthasol (Merck), rats received a firm toe pinch to assure unconsciousness. A 5-6 mm incision is made through the abdominal wall beneath the rib cage to expose the heart. An injection needle was inserted into the left ventricle and the right atrium was punctured to allow first an infusion of PBS and second 4% PFA. The rat was decapitated and its brain collected and preserved in 4% PFA. Coronal brain slices of 50 µm were made using a vibratome (Leica VT1000S) and preserved in PBS + 0.01% sodium azide to prevent bacterial proliferation.

Slices were rinsed with PBS three times for ten minutes and left in blocking solution (1X PBS + 0.1% TritonX + 5% goat/donkey serum) for at least one hour. The first antibody (1:750 mouse anti NeuN + 1:1000 rabbit anti GFP) was left on incubation overnight at 4°C. The next day, the slices were left to adjust to room temperature, rinsed with PBS three times for ten minutes and the secondary antibody (1:400 Donkey anti rabbit 488 + 1:400 Donkey anti mouse 647) was added. After two hours, the slices were washed in PBS three times for ten minutes and mounted in glass slices using Mowiol. Imaging of the slices was performed with a confocal microscope (Leica Axiovert 200M) and images were processed and edited in ImageJ (Rueden et al., 2017).

Data preprocessing

The ΔF/F calculation was performed by adjusting the violet channel (405nm) as a baseline using the formula:

$$\frac{\Delta \mathrm{F}}{\mathrm{F}} = \frac{\mathrm{Signal}_{490\mathrm{nm}} - \mathrm{Signal}_{405\mathrm{nm}}}{\mathrm{Signal}_{405\mathrm{nm}}}$$

The data had outliers removed using the `isoutlier` function in MATLAB 2018b – defined by data points more than three median absolute deviations away from the median and often observed in the start of the session due to bleaching. Manual removal of outliers also occurs in instances when the cable got disconnected in the middle of a session. All processing steps were done using custom scripts in MATLAB (Mathworks) with the Statistics and Machine Learning toolbox. The scripts can be found on GitHub (https://github.com/sybrendekloet).

Statistical analysis

In the analysis, we usually used rats as a unit of measurement – comparing GCaMP signal within the same rat during different stages of training – which reduces the required sample size in order to have sufficiently powered results. We used eucledian distances as a quantitative measurement of the difference between two curves with the function `pdist2` in MATLAB. When comparing signals of the same rat in different stages, we chose paired statistics (either paired t-tests or the non-parametric Wilcoxon signed rank test) and when comparing independent samples (e.g. dmPFC against vmPFC), an independent sample t-test was used. The statistics were performed in SPSS 25 (IBM, USA) and GraphPad Prism 6 (GraphPad Software, USA).

3 Results

Immunohistochemistry validation

In order to validate the photometry results obtained, we needed to demonstrate that the fluorescence was originated from GCaMP expression in the brain regions of interest. In the viral construct, a non-specific promoter was chosen – Synapsin (**Figure 4A**) – in order to affect all neurons around the area of the injection, either dmPFC (AP +2.76mm; ML ±1.49 mm; DV −2.94) or vmPFC (AP +2.76 mm; ML ±0.5 mm; DV −4.65 mm) (**Figure 4B**). Injections were done unilaterally in the right hemisphere and the fiber implant was inserted in the same location. Expression of GCaMP6 in the correct brain region was observed for all rats (**Figure 4C** and **Supplementary Figure 1**), the NeuN staining was nicely colocalized with GCaMP and with no signs neuronal death. The virus expression spread around the injection, but the fiber placement was correct, which means that the signal detected was coming from the brain regions of interest (**Figure 4D**). Because all rats had good photometry signal related to GCaMP in the proper location and with no signs of histological anomalies, no rats were excluded from the sample. In total, there were 6 rats in the dmPFC group and 5 rats in the vmPFC group.

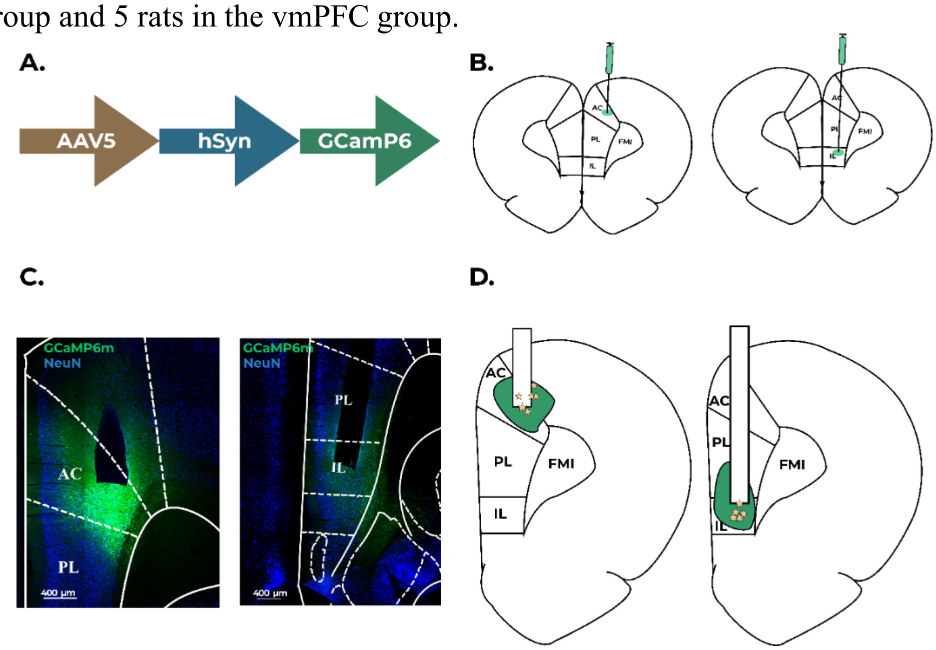

Figure 4. Viral GCaMP expression elicits quantifiable calcium transients. A) Viral construct AAV5-humanSynapsin-GCaMP6. B) Placement of virus injection in dmPFC and vmPFC, respectively. C) Examples of fiber placement and GCaMP6 expression of one rat for each group. The difference in GCaMP expression resulted in different intensity of photometry signal, which had to be accounted

for in the analysis. D) Average expression of GCaMP6 (green blob) and placement of fiber for every rat in each group (orange stars).

Behavioral data

In order to assess if the surgeries differently impacted the cognitive ability of the rats, we compared the progression of animals throughout the learning stages (**Figure 6**). Except for the performance of a single rat in stage 8, there is no major difference between performance of vmPFC and dmPFC - **S1**: $F = 2.069$, $\alpha = 0.193$ (n.s.), $df = 7$; **S2**: $F = 1.146$ $\alpha = 0.320$ (n.s.), $df = 7$; **S3**: $F = 0.749$, $\alpha = 0.415$ (n.s.), $df = 7$; **S4**: $F = 5.531$, $\alpha = 0.051$ (n.s.), $df = 7$; **S5**: $F = 0.099$, $\alpha = 0.762$ (n.s.), $df = 7$; **S6**: $F = 0.728$, $\alpha = 0.422$ (n.s.), $df = 7$; **S7**: $F = 0.816$, $\alpha = 0.397$ (n.s.), $df = 7$; **S8**: $F = 7.378$, $\alpha = 0.030$, $df = 7$; **S9**: $F = 0.005$, $\alpha = 0.945$ (n.s.), $df = 7$. When the outlier is removed from the analysis, there is no significant difference between both groups – **S8**: $F = 1.252$, $\alpha = 0.306$ (n.s.), $df = 6$. This demonstrates that the surgeries did not affect their performances in a distinct manner. The progression from one learning stage to another was defined by the animal doing over 50 trials with greater than 80% accuracy and less than 40% omissions. Learning progression was more difficult in early stages (S1-S3) because the animals need to learn the task contingencies, then became easier in middle stages (S4-S7) and spiked in difficulty again when the animals only have 1.5 or 1 second to respond correctly (S8-S9). This shows that there is no significant difference in progression between dmPFC and vmPFC and that the task difficult is reflected in the number of sessions that the animals needed to advance the learning stages.

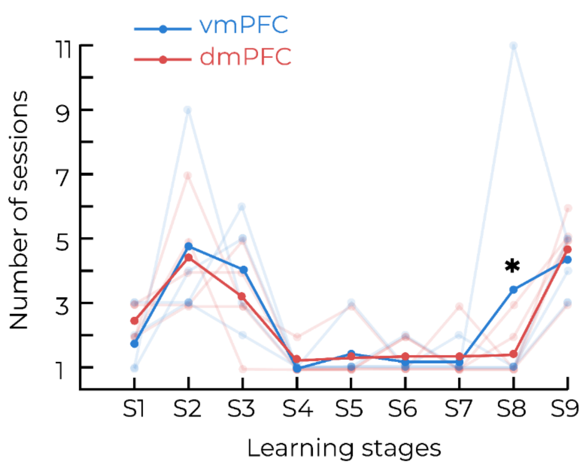

Figure 6. Rats in dmPFC and vmPFC groups progress through the learning stages at the same rate. **S1**: $F = 2.069$, $\alpha = 0.193$ (n.s.), $df = 7$; **S2**: $F = 1.146$ $\alpha = 0.320$ (n.s.), $df = 7$; **S3**: $F = 0.749$, $\alpha = 0.415$ (n.s.), $df = 7$; **S4**: $F = 5.531$, $\alpha = 0.051$ (n.s.), $df = 7$; **S5**: $F = 0.099$, $\alpha = 0.762$ (n.s.), $df = 7$; **S6**: $F = 0.728$, $\alpha = 0.422$ (n.s.), $df = 7$; **S7**: $F = 0.816$, $\alpha = 0.397$ (n.s.), $df = 7$; **S8**: $F = 7.378$, $\alpha = 0.030$, $df = 7$; **S9**: $F = 0.005$, $\alpha = 0.945$ (n.s.), $df = 7$. When the outlier is removed from the analysis, there is no significant difference between both groups – **S8**: $F = 1.252$, $\alpha = 0.306$ (n.s.), $df = 6$.

To investigate the development of neuronal activity throughout all the learning stages, we chose a single illustrative rat for dmPFC and vmPFC. The photometry data was synced either in terms of trial start or response time – since after the animal starts a trial, it may respond at different times, before or after the cue light turns on, or not respond at all. The data is shown in terms of a heatmap with the activity of every trial throughout all stages, which shows the overall shift of activity or by line drawings of S3/S9 (mean ± SEM), chosen as examples of an early and a late stage of learning respectively.

In the later stage of learning (S9), the dmPFC seems to become more active one second before and a few seconds after the trial start (**Figures 7A** and **7C**) compared to an early stage (S3). This brain region also seems to become less active a few seconds before response in later stages compared to earlier ones (**Figures 7B** and **7D**).

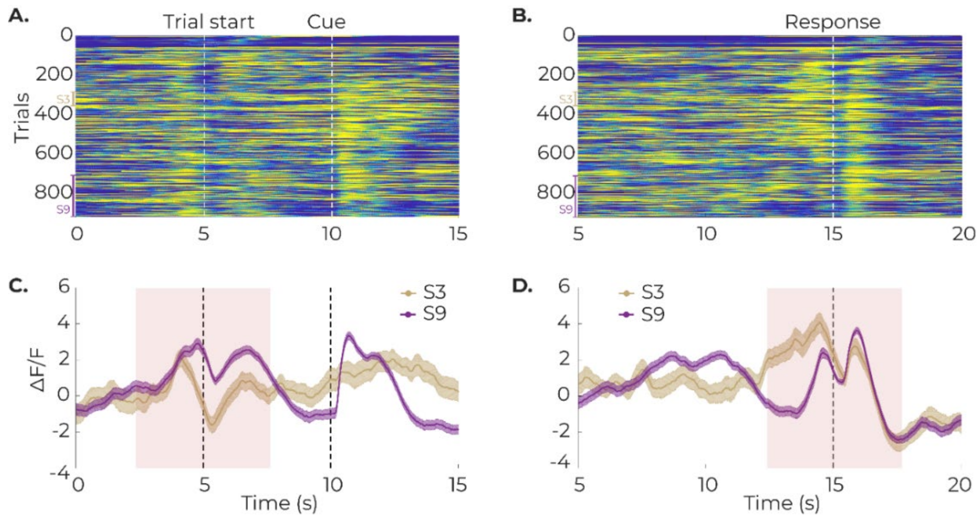

Figure 7. Neuronal activity patterns change according to learning in dmPFC. A) Heatmap of activity synced at trial start as the animal progresses through all learning stages. B) Heatmap of activity synced at response time as the animal progresses through all learning stages. C) Comparison of activity synced at trial start in an early stage of learning (S3) and a late stage of learning (S9). D) Comparison of activity synced at response time in an early stage of learning (S3) and a late stage of learning (S9).

On the other hand, we observe a difference development of activity in the vmPFC: this brain region appears to become less active after cue presentation (**Figures 8A** and **8C**) and also less active before and after response time in later stages (**Figures 8B** and **8D**). We conclude that there is a distinct pattern of development of neuronal activity in the dmPFC and vmPFC as each rat progresses through the learning stages.

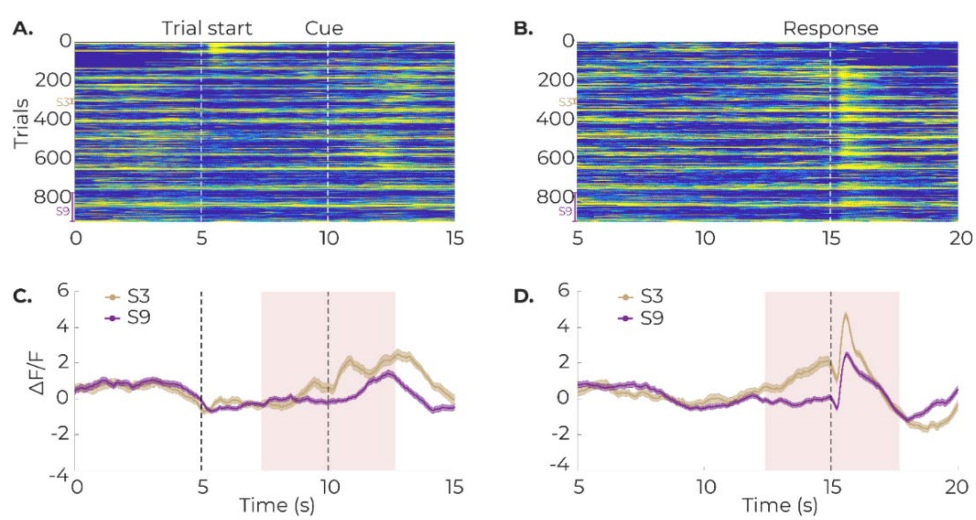

Figure 8. Neuronal activity patterns change according to learning in vmPFC. A) Heatmap of activity synced at trial start as the animal progresses through all learning stages. B) Heatmap of activity

synced at response time as the animal progresses through all learning stages. C) Comparison of activity synced at trial start in an early stage of learning (S3) and a late stage of learning (S9). D) Comparison of activity synced at response time in an early stage of learning (S3) and a late stage of learning (S9).

To understand if this pattern of signal evolution was consistent throughout all learning stages, we calculated an information distance matrix. Information distance is defined as the area between two curves (**Figure 9A**), and it provides a quantitative measurement of change in signal from one stage to the other. We notice a clear trend of increased activity in dmPFC around trial start (**Figure 9B**), indicating a higher engagement of this brain region as a function of the task difficulty. There is a noticeable decrease in dmPFC engagement around response time, especially around the later stages, such as 7, 8 and 9 (**Figure 9C**). When comparing activity of vmPFC around the cue presentation time window, there is a perceptible disengagement of this brain region after stage 2 (as compared to all other stages), but not a noticeable difference amongst later stages. (**Figure 9D**). In the response time window, there is a notable decrease in activity after stage 2 as well, with a strong similarity of signal between stages 3, 4, 5 and 6 (**Figure 9E**).

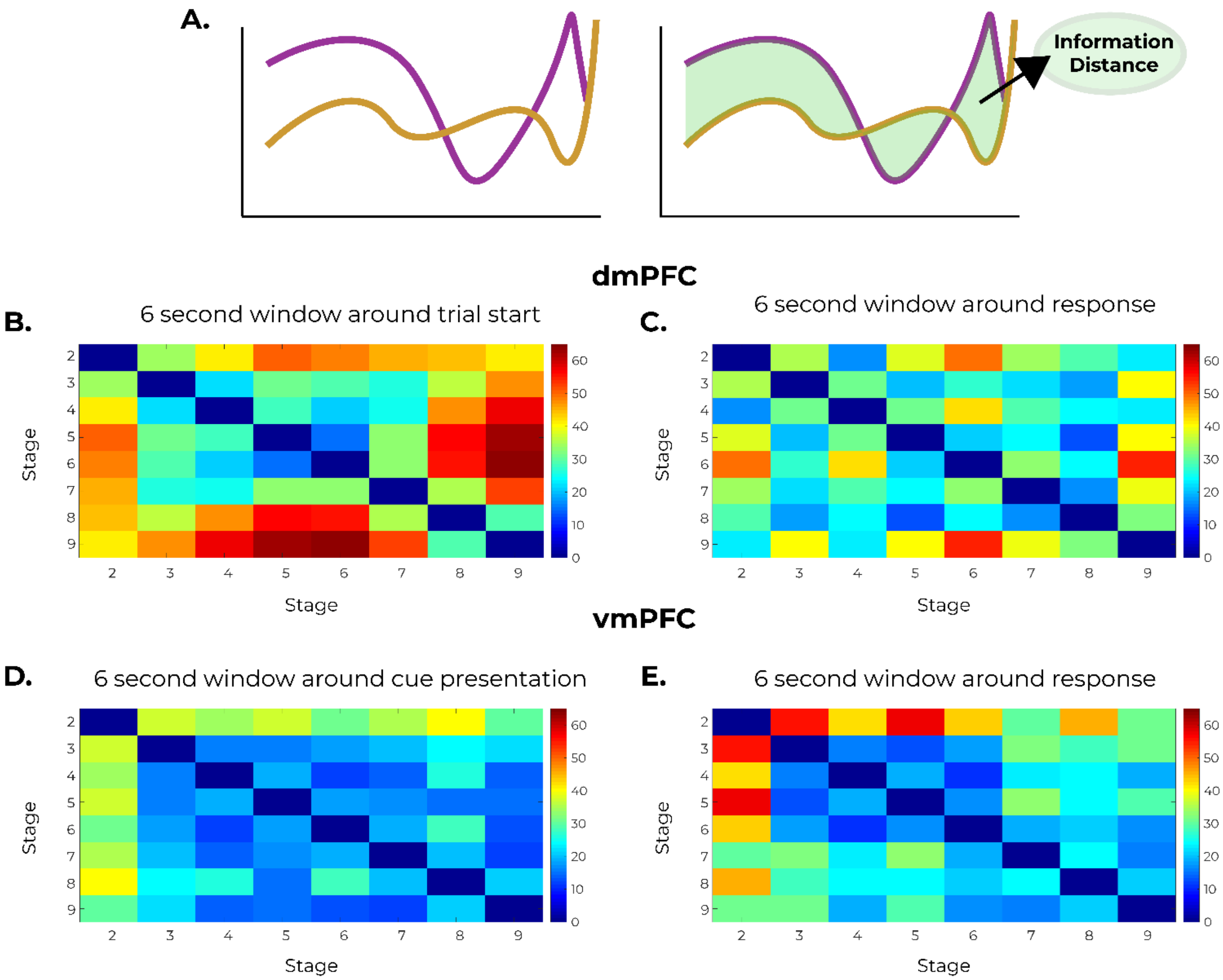

Figure 9. Information distance as a measurement of signal evolution between learning stages. A) Definition of information distance – the area described between two curves. B) Information distance matrix 6 seconds around trial start for dmPFC. C) Information distance matrix 6 seconds around

response time for dmPFC. D) Information distance matrix 6 seconds around cue presentation for dmPFC. E) Information distance matrix 6 seconds around response time for vmPFC.

When observing a time window 3 seconds after the trial start, there is a noticeable decrease in activity in the vmPFC compared to dmPFC (**Figure 10A**); S4 – $t(71) = 2.172$, $p < 0.05$; S6 – $t(71) = 2.029$, $p < 0.05$; S7 – $t(71) = 2.038$, $p < 0.05$; S9 – $t(71) = 3.105$, $p < 0.005$. We observed the development of completely different signals throughout the learning stages depending on the time window. When assessing the maximum df/f value for all trials in stages 3 and 9, we observe no clear trend in dmPFC (**Figure 10B**), although two rats in this group have a significant difference in signal between stages using Wilcoxon signed rank test: dm1 – Mdn = 0.915, z = 3888, $p < 0.001$; dm2 – Mdn = -1.293, z = -2777, $p < 0.005$. However, there is a noticeable decrease in maximum signal in vmPFC between an early and a late stage of learning, consistent among all rats (**Figure 10C**). There are also two rats in this group with a statistically significant change in signal. vm1 – Mdn = -2692, z = -5725, $p < 0.0001$; vm2 – Mdn = -1.632, z = -15600, $p < 0.0001$. This result indicates a different progression of signal evolution in dmPFC and vmPFC throughout the learning stages depending on the time window of choice.

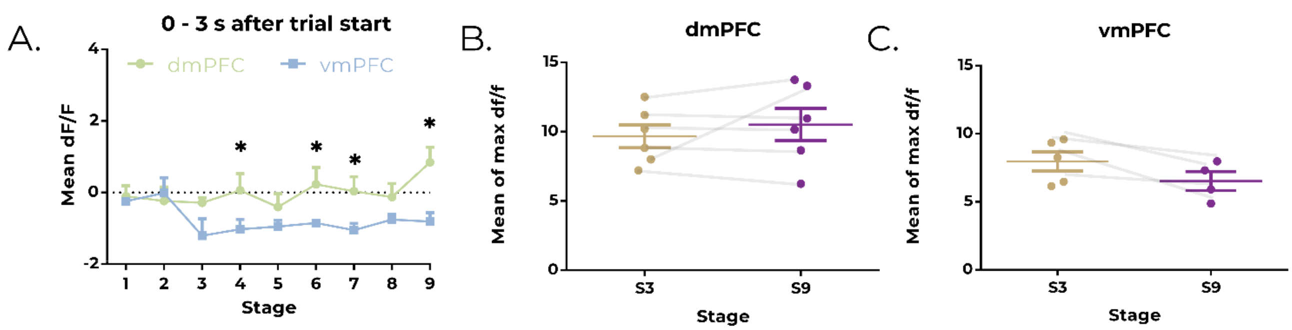

Figure 10. The dmPFC and vmPFC develop different training-related patterns of activity during particular time windows in the 5CSRTT. A) Comparison of signal evolution between dmPFC and vmPFC 0-3 seconds after trial start. Asterisks indicate an independent sample t-test p value less than 0.05. B) Comparison of maximum peak average between S3 and S9 in dmPFC. C) Comparison of maximum peak average between S3 and S9 in vmPFC.

Since the selection of time windows is intrinsically arbitrary, we next decide to compare the time window with the greatest behavioral relevance – the period in which the animal is withholding a response before the cue light goes off (**Figure 11A**). The average activity of dmPFC increases during the waiting period before cue presentation (ITI) compared to 1.5-3 seconds before the start of the trial in later stages (**Figure 11B**) - S3 – $t(9) = 3.366$, $p<0.01$; S4 – $t(9) = 2.570$, $p<0.05$; S5 – $t(9) = 3.026$, $p<0.05$; S6 – $t(8) = 2.530$, $p<0.05$; S7 – $t(8) = 3.036$, $p<0.05$; S9 – $t(8) = 2.555$, $p<0.05$. Contrarily, the vmPFC tends to be more active during the waiting period in early stages compared to baseline – S2 – $t(6) = 2.938$, $p < 0.05$; S3 – $t(8) = 4.1331$, $p < 0.05$ – however that effect subsides in later stages of learning (**Figure 11C**). This corroborates the idea of a distinct development of activity of dmPFC and vmPFC throughout the learning stages.

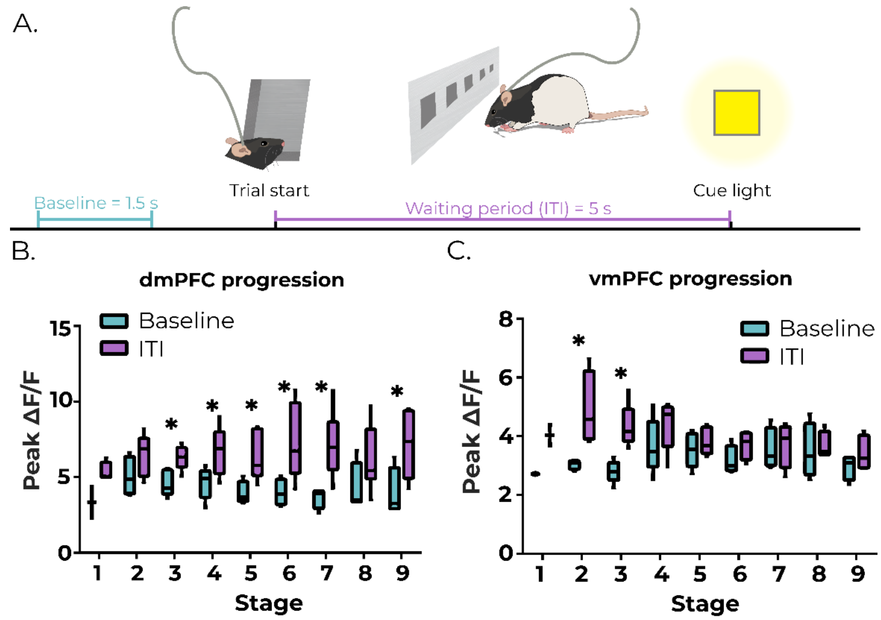

Figure 11. The dmPFC and vmPFC develop different training-related patterns of activity during the waiting period for the cue light. A) Definition of baseline (1.5 – 3 seconds before the trial start) and ITI. B) Changes in area of peaks in dmPFC comparing baseline and ITI. C) Changes in area of peaks in vmPFC comparing baseline and ITI. Asterisks indicate a paired t-test p value less than 0.05.

4 Discussion

Our working hypothesis were supported: (1) there were distinct evolutions of patterns in dmPFC and vmPFC; (2) brain activity changed over time as a result of task-learning and (3) vmPFC transient activity decreased as a result of learning. However, dmPFC activity increased in certain periods of the 5CSRTT as the rat progressed through the learning stages, indicating that this brain region is not involved in the habituation of the task. The vmPFC is involved in attention selection and inhibitory control (Uran et al., 2017) which might become less important as the visuospatial task becomes more habitual to the rat. On the other hand, the dmPFC is involved in motor coordination and planning of movement (Hyman et al., 2013) which might necessitate a higher level of activity because of the shortening of the stimulus duration.

Limitations of 5CSRTT

The 5-choice serial-reaction time task proports to assess spatial and temporal attentional states in the animal. It is important to remember that attention or any other cognitive process are not directly observable or quantifiable. Therefore, the study of attention with animal models depends on the expression of behavior of the animal which can then be used to indirectly assess the cognitive process underneath: in this paradigm, accuracy is a proxy measure of attention and premature responses are an indirect measure of impulsivity.

However, omissions can often happen not due the lack of attention, but for different biases. For instance, we observed that some rats had a strong preference to attend to just 3 or 4 holes, usually omitting all the trials from the always-unattended holes. If omissions are used as a proxy for attention, these instances of strong bias towards certain holes comprise an important confounding effect. Other confounding factors include: different stress responses because of handling; the rats become more satiated and therefore less motivated to complete the task as the session progresses; and as the rats become better at the task, they are more likely to use a time-dependent strategy instead of fully diverting attention to the task – therefore high accuracy results may not be actually representative of sustained attentional states, but of other cognitive processes (Leite-Almeida et al., 2013).

Limitations of fiber photometry

Fiber photometry has many advantages compared to other calcium imaging methods, such as two-photon microscopy and the miniscope (**Table 3**). FP is cheaper and technically easier to implement, the cable is light-weight and flexible thus allowing the animal to move more freely, and it is capable to measure single photons since it is a system based on fiber optics. (Cui et al., 2014).

Table 3. Comparison of modern *in vivo* calcium imaging technologies.

Parameter	Fiber Photometry	Miniscope	Two-photon Microscopy
Sensitivity	++ (single photons)	+ Higher background noise than two-photon micros-copy	+
Cellular Resolution	- No cellular resolution	+ (soma)	++ (soma and dendrites)
Freely moving	Yes	Yes	No
Brain damage caused by implant	Less significant Fiber is 0.2-0.4 µm	Significant GRIN lens is 0.5-1 mm	Significant GRIN lens is 0.5 - 1 mm
Can be used underwater	Yes	No	No
Light scattering	+++ (shorter wavelengths for excitation)	++	+ (longer wavelengths for excitation)
Price	$ (cheapest)	$$	$$$ (most expensive)

Data adapted from Girven & Sparta (2017).

However, the main limitation of FP is its lack of cellular resolution – which means that it measures all the neurons that express GCaMP. Though the viral construct can be specific for particular neuronal types, it is important to realize a lot of information is lost. For example, a baseline FP signal may represent a population of cells baseline active for all timepoints or fractions of the neuronal population spiking in activity – both scenarios yield the same signal, but they have completely different biological significances and interpretations (**Figure 12**).

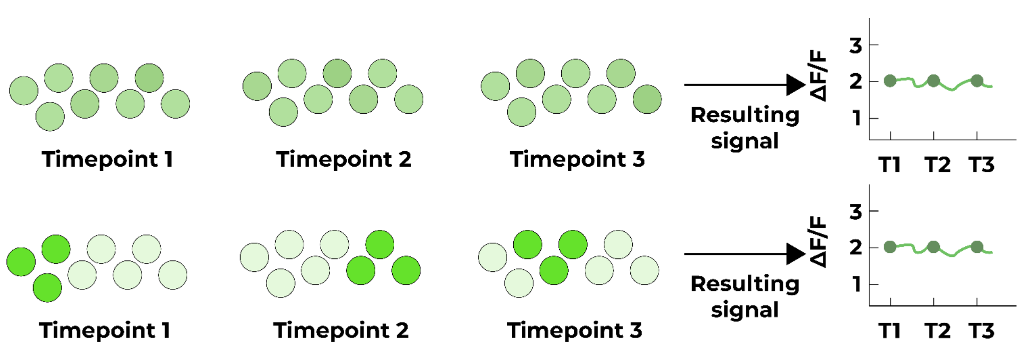

Figure 12. Different patterns of neuronal activation may yield similar fiber photometry signals. The lack of cellular resolution is one of the main limitations of fiber photometry.

Another important consideration is that, due to light scattering increasing with the square of the distance, only a very small volume of brain cells around the tip of the fiber are detectable, only 200 µm (Pisanello et al., 2018). This entails that, if a neuronal population is sparse in the cortex, the FP signal might not be usable, and another technique that uses longer wavelengths for excitation, such as two-photon, might be more appropriate. Furthermore, different rats often have different baseline signals due to different expression of GCaMP – this complicates the interpretation of data, since similar patterns of neuronal activity may yield completely different signals.

In this preliminary investigate study, we chose a non-specific promoter in the viral construct. This means that both excitatory and inhibitory neurons in the PFC were transfected and greatly increases the difficulty of data interpretation, since the increase GCaMP fluorescence/neuronal activation may be related to an increase of inhibitory or excitatory neurons. In the result section, we chose to specify that an increase in fluorescence was related to 'an increase in neuronal activity'. It is known that around 90% of neurons in the rodent PFC are pyramidal/glutamatergic (Riga et al., 2014), and we hypothesize that these neurons drive a greater percentage of the signal observed. However, the proportion of activity for each neuronal type and how they relate to behavior remains unclear.

Big picture and next steps

Attention is a neurological construct which is comprised by complex cognitive processes related to the detection and organization of sensory input. It can be divided into different subcategories of attention: orienting, selective attention, sustained attention and divided attention (Mar & Dalley, 2010). It mediates other cognitive processes such as memory formation and learning; consequently, aberrations in attention are often associated with neurological disorders. Therefore, by methodically studying attention in animal models, it is possible to obtain important insights on the underpinnings of diseases and how they can be affected by treatments (Arnold et al., 2003).

This study is an important first step in trying to understand the brain mechanisms related to attention and how they change during the process of learning a task. Fiber photometry data reveals a richness in distinct development of brain activity in dmPFC and vmPFC. It is possible that different cognitive processes take place during the different stages of learning – and that this could be generalized to other forms of learning other than visuospatial attention.

For future studies, it would be enlightening to use intervention techniques in combination with fiber photometry to try to understand more clearly the roles of each brain region and how they change according to the process of learning the attentional task. The use of specific viral promoters to understand the role of different neuronal subtypes in the PFC would also be very elucidating. Furthermore, we could use vITI and vSD trials to disrupt the habitual nature of the task — which could provide more clear mechanistic underpinnings of the role of dmPFC and vmPFC in learning. We also aim to use automated video-tracking software with Machine Learning using DeepLabCut (Mathis et al., 2018) which would allow the separation of data that emerge from different types of behaviors (**Supplementary Figure 2**) and permit a much more precise analysis of the development of brain activity.

5 Conflicts of Interest

The authors declare that the research was conducted in the absence of any commercial or financial relationships that could be construed as a potential conflict of interest.

6 Author Contributions

HM obtained funding for the study. HM and SK designed the study. SK performed surgeries and perfusion. SK and VB executed FP recordings. SK developed custom MATLAB scripts for data analysis. HM, VB and SK analyzed the data. VB wrote the manuscript with input from the other authors.

7 Funding

This study was funded by the Netherlands Organization for Scientific Research (NWO; 917.76.360, 912.06.148; one VICI grant), ERC StG "BrainSignals," the Dutch Fund for Economic Structure Reinforcement (FES, 0908 "NeuroBasic PharmaPhenomics project"), EU 7th Framework Programme (HEALTH-F2-2009-242167 "SynSys" and agreement no. 604102 "Human Brain Project").

8 Acknowledgements

We would like to thank Guilherme Ribeiro for helping during recording and training of animals, Huub Terra and Bastian Bruinsma for their technical assistance, and the Dutch Neuroscience Meeting (DNM19), which allowed us to present this information in a poster form in order to receive input and feedback (**Supplementary Figure 3**).

VB personally thanks the institutions that funded his studies: Vrije Universiteit (Vrije Universiteit Fellowship Programme – VUFP and Holland Scholarship Program – HSP), Nuffic Neso (Orange Tulip Scholarship), Schuurman Schimmel and Groesbeek-Assenbroek (grants for living expenses).

9 References

Alexander Mathis, Pranav Mamidanna, Kevin M. Cury, Taiga Abe, V. N. M. M. W. M. and M. B. (2018). DeepLabCut: markerless pose estimation of user-defined body parts with deep learning. *Nature Neuroscience*, *21*, 1281–1289. https://doi.org/10.1038/s41593-018-0209-y

Ambrogi Lorenzini, C., Bucherelli, C., Giachetti, A., & Tassoni, G. (1987). Spontaneous and conditioned behavior of Wistar and Long Evans rats. *Archives Italiennes de Biologie*, *125*(2), 155–170. Retrieved from http://www.ncbi.nlm.nih.gov/pubmed/3662730

Augustine, G. J., Charlton, M. P., & Smith, S. J. (1985). Calcium entry and transmitter release at voltage-clamped nerve terminals of squid. *J. Physiol*, *361*, 163–181. Retrieved from https://www.ncbi.nlm.nih.gov/pmc/articles/PMC1193058/pdf/jphysiol00565-0174.pdf

Barker, D. J., Sanabria, F., Lasswell, A., Thrailkill, E. A., Pawlak, A. P., Killeen, P. R., … Killeen, P. (2010). Brief light as a practical aversive stimulus for the albino rat. *Behav Brain Res*, *214*(2), 402–408. https://doi.org/10.1016/j.bbr.2010.06.020

Barnes, T. D., Kubota, Y., Hu, D., Jin, D. Z., & Graybiel, A. M. (2005). Activity of striatal neurons reflects dynamic encoding and recoding of procedural memories. https://doi.org/10.1038/nature04053

Boekhoudt, L., Voets, E. S., Flores-Dourojeanni, J. P., Luijendijk, M. C., JMJ Vanderschuren, L., & Adan, R. A. (2016). Chemogenetic Activation of Midbrain Dopamine Neurons Affects Attention, but not Impulsivity, in the Five-Choice Serial Reaction Time Task in Rats. *Nature Publishing Group*, *42*, 1315–1325. https://doi.org/10.1038/npp.2016.235

Carlén, M. (2017). What constitutes the prefrontal cortex? *Science*, *358*(6362), 478–482. https://doi.org/10.1126/science.aan8868

Carr, M. R., de Vries, T. J., & Pattij, T. (2018). Optogenetic and chemogenetic approaches to manipulate attention, impulsivity and behavioural flexibility in rodents. *Behavioural Pharmacology*, *29*(7), 560–568. https://doi.org/10.1097/FBP.0000000000000425

Carter, M., & Shieh, J. (2015). Electrophysiology. *Guide to Research Techniques in Neuroscience*, 89–115. https://doi.org/10.1016/B978-0-12-800511-8.00004-6

Chen, T.-W., Wardill, T. J., Sun, Y., Pulver, S. R., Renninger, S. L., Baohan, A., … Kim, D. S. (2013). *Ultra-sensitive fluorescent proteins for imaging neuronal activity* (Vol. 499). Retrieved from http://www.nature.com/authors/editorial_policies/license.html#terms

Chudasama, Y., Passetti, F., Rhodes, S. E. V, Lopian, D., Desai, A., & Robbins, T. W. (2003). Dissociable aspects of performance on the 5-choice serial reaction time task following lesions of the dorsal anterior cingulate, infralimbic and orbitofrontal cortex in the rat: differential effects on selectivity, impulsivity and compulsivity. *Behavioural Brain Research*, *146*, 105–119. https://doi.org/10.1016/j.bbr.2003.09.020

Coutureau, E., & Killcross, S. (2003). Inactivation of the infralimbic prefrontal cortex reinstates goal-directed responding in overtrained rats. *Behavioural Brain Research*, *146*, 167–174. https://doi.org/10.1016/j.bbr.2003.09.025

Cui, G., Jun, S. B., Jin, X., Luo, G., Pham, M. D., Lovinger, D. M., … Costa, R. M. (2014). Deep brain optical measurements of cell type-specific neural activity in behaving mice. *Nature Protocols*, *9*(6), 1213–1228. https://doi.org/10.1038/nprot.2014.080

Dalley, J. W., Cardinal, R. N., & Robbins, T. W. (2004). Prefrontal executive and cognitive functions in rodents: Neural and neurochemical substrates. In *Neuroscience and Biobehavioral Reviews* (Vol. 28, pp. 771–784). https://doi.org/10.1016/j.neubiorev.2004.09.006

De Bruin, J. P. C., Sgnchez-Santed, F., Heinsbroek, R. P. W., Donker, A., & Postmes, P. (1994). *Brain research: A behavioural analysis of rats with damage to the medial prefrontal cortex using the morris water maze: evidence for behavioural flexibility, but not for impaired spatial navigation*. Retrieved from https://ac.els-cdn.com/0006899394902437/1-s2.0-0006899394902437-main.pdf?_tid=21a4b61e-abd3-49a7-be78-a1e3a4a417c1&acdnat=1551341557_4692f56ad90353a3b671427e249fd65a

De Wit, S., Kosaki, Y., Walter Balleine, B., & Dickinson, A. (2006). Behavioral/Systems/Cognitive Dorsomedial Prefrontal Cortex Resolves Response Conflict in Rats. https://doi.org/10.1523/JNEUROSCI.5175-05.2006

Domenech, P., & Koechlin, E. (2015). Executive control and decision-making in the prefrontal cortex. *Current Opinion in Behavioral Sciences*, *1*, 101–106. https://doi.org/10.1016/j.cobeha.2014.10.007

Donnelly, N A, Holtzman, T., Rich, P. D., Nevado-Holgado, A. J., & Fernando, A. B. P. (2014). Oscillatory Activity in the Medial Prefrontal Cortex and Nucleus Accumbens Correlates with Impulsivity and Reward Outcome. *PLoS ONE*, *9*(10), 111300.

https://doi.org/10.1371/journal.pone.0111300

Donnelly, Nicholas A., Paulsen, O., Robbins, T. W., & Dalley, J. W. (2015). Ramping single unit activity in the medial prefrontal cortex and ventral striatum reflects the onset of waiting but not imminent impulsive actions. *European Journal of Neuroscience*, *41*(12), 1524–1537. https://doi.org/10.1111/ejn.12895

Erin Campbell, C. J., Marchant, N. J., & Campbell, E. J. (2018). The use of chemogenetics in behavioural neuroscience: receptor variants, targeting approaches and caveats. *British Journal of Pharmacology*, *175*, 994. https://doi.org/10.1111/bph.14146

Fisher, B. M. (2018). *Role of prefrontal cortex and cholinergic modulation in attentional performance in rats*. University of Cambridge. Retrieved from https://doi.org/10.17863/CAM.21750

Frank, G. A.-G., Kentaroh, W. O., Michael, T., Lippert, T., Arias-Gil, G., Ohl, F. W., … Lippert, M. T. (2016). Measurement, modeling, and prediction of temperature rise due to optogenetic brain stimulation, *3*(4), 45007. https://doi.org/10.1117/1.NPh.3.4.045007

Fuster, J. M. (2015). *Anatomy of the Prefrontal Cortex*. *The Prefrontal Cortex*. https://doi.org/10.1016/B978-0-12-407815-4.00002-7

Gabbott, P. L. A., Warner, T. A., Jays, P. R. L., Salway, P., & Busby, S. J. (2005). Prefrontal cortex in the rat: Projections to subcortical autonomic, motor, and limbic centers. *Journal of Comparative Neurology*, *492*(2), 145–177. https://doi.org/10.1002/cne.20738

Girven, K. S., & Sparta, D. R. (2017). Probing Deep Brain Circuitry: New Advances in in Vivo Calcium Measurement Strategies. *ACS Chemical Neuroscience*. https://doi.org/10.1021/acschemneuro.6b00307

Gunaydin, L. A., Grosenick, L., Finkelstein, J. C., Kauvar, I. V, Fenno, L. E., Adhikari, A., … Deisseroth, K. (2014). Natural Neural Projection Dynamics Underlying Social Behavior. *Cell*, *157*, 1535–1551. https://doi.org/10.1016/j.cell.2014.05.017

H. Moore Arnold, John P. Bruno, and M. S. (2003). Assessment of Sustained and Divided Attention in Rats. *Current Protocols in Neuroscience*, *22*(1), 8.5E.1-8.5E.13. https://doi.org/10.1002/0471142301.ns0805es22

Hardung, S., Epple, R., Jäckel, Z., Eriksson, D., Uran, C., Senn, V., … Diester, I. (2017). A Functional Gradient in the Rodent Prefrontal Cortex Supports Behavioral Inhibition. *Current Biology*, *27*(4), 549–555. https://doi.org/10.1016/j.cub.2016.12.052

Heidbreder, C. A., & Groenewegen, H. J. (2003). The medial prefrontal cortex in the rat: evidence for a dorso-ventral distinction based upon functional and anatomical characteristics. https://doi.org/10.1016/j.neubiorev.2003.09.003

Higgins, G. A., & Silenieks, L. B. (2017). Rodent test of attention and impulsivity: The 5-choice serial reaction time task. *Current Protocols in Pharmacology*, *2017*(September), 5.49.1-5.49.34. https://doi.org/10.1002/cpph.27

Hoseok Kim, A., Wang, X., Deisseroth, K., Carlé Correspondence, M., Kim, H., & Carlé, M. (2016). Prefrontal Parvalbumin Neurons in Control of Attention In Brief Prefrontal Parvalbumin Neurons in Control of Attention. *Cell*, *164*, 208–218. https://doi.org/10.1016/j.cell.2015.11.038

Hyman, J. M., Whitman, J., Emberly, E., Woodward, T. S., & Seamans, J. K. (2013). Action and Outcome Activity State Patterns in the Anterior Cingulate Cortex. *Cerebral Cortex*, *23*, 1257–1268. https://doi.org/10.1093/cercor/bhs104

Junich Nakai, M. O. & K. I. (2001). *The measurement of intracellular Ca 2+ concentration, [Ca 2+] i*. Retrieved from http://biotech.nature.com

Kesner, R. P., & Churchwell, J. C. (2011). An analysis of rat prefrontal cortex in mediating executive function. https://doi.org/10.1016/j.nlm.2011.07.002

Koike, H., Demars, M. P., Short, J. A., Nabel, E. M., Akbarian, S., Baxter, M. G., & Morishita, H. (2015). Chemogenetic Inactivation of Dorsal Anterior Cingulate Cortex Neurons Disrupts Attentional Behavior in Mouse. *Neuropsychopharmacology*, *41*, 1014–1023. https://doi.org/10.1038/npp.2015.229

Kupferschmidt, D. A., Juczewski, K., Cui, G., Johnson, K. A., & Lovinger, D. M. (2017). Parallel, but Dissociable, Processing in Discrete Corticostriatal Inputs Encodes Skill Learning. *Neuron*, *96*(2), 476-489.e5. https://doi.org/10.1016/j.neuron.2017.09.040

Leite-Almeida, H., Melo, A., Pêgo, J. M., Bernardo, S., Milhazes, N., Borges, F., … Cerqueira, J. J. (2013). Variable delay-to-signal: a fast paradigm for assessment of aspects of impulsivity in rats. *Frontiers in Behavioral Neuroscience*, *7*(October), 1–9. https://doi.org/10.3389/fnbeh.2013.00154

Luchicchi, A., Mnie-Filali, O., Terra, H., Bruinsma, B., de Kloet, S. F., Obermayer, J., … Mansvelder, H. D. (2016). Sustained Attentional States Require Distinct Temporal Involvement of the Dorsal and Ventral Medial Prefrontal Cortex. *Frontiers in Neural Circuits*, *10*, 70. https://doi.org/10.3389/fncir.2016.00070

Maddux, J.-M., & Holland, P. C. (2011). Effects of dorsal or ventral medial prefrontal cortical lesions on five-choice serial reaction time performance in rats. https://doi.org/10.1016/j.bbr.2011.02.031

Mar, A. C., & Dalley, J. W. (2010). Cognition: Attention and Impulsivity. *Encyclopedia of Behavioral Neuroscience*, 262–271. https://doi.org/https://doi.org/10.1016/B978-0-08-045396-5.00003-8

Muir, J. L., Everitt, B. J., & Robbins, T. W. (1996). The cerebral cortex of the rat and visual attentional function: Dissociable effects of mediofrontal, cingulate, anterior dorsolateral, and parietal cortex lesions on a five-choice serial reaction time task. *Cerebral Cortex*, *6*(3), 470–481. https://doi.org/10.1093/cercor/6.3.470

Otani, S. (2004). *Prefrontal Cortex - From Synaptic Plasticity to Cognition*. *Neurosciences*. New York: Kluwer Academic Publishers. https://doi.org/10.1007/b111822

Panicker, A. (2016). *Assessment of the Functional Relevance of the Claustrum in Attention Item Type* *dissertation*. Retrieved from http://hdl.handle.net/10713/5447

Passetti, F., Chudasama, Y., & Robbins, T. W. (2002). The frontal cortex of the rat and visual attentional performance: dissociable functions of distinct medial prefrontal subregions. *Cerebral Cortex (New York, N.Y. : 1991)*, *12*(12), 1254–1268. https://doi.org/10.1093/cercor/12.12.1254

Pisanello, M., Pisano, F., Hyun, M., Maglie, E., Balena, A., De Vittorio, M., … Pisanello, F. (2018). Analytical and empirical measurement of fiber photometry signal volume in brain tissue, *i*, 1–41. Retrieved from http://arxiv.org/abs/1807.03023

Ragozzino, M. E., Wilcox, C., Raso, M., & Kesner, R. P. (1999). Involvement of rodent prefrontal cortex subregions in strategy switching. *Behavioral Neuroscience*, *113*(1), 32–41. https://doi.org/10.1037/0735-7044.113.1.32

Resendez, S. L., & Stuber, G. D. (2015). In vivo Calcium Imaging to Illuminate Neurocircuit Activity Dynamics Underlying Naturalistic Behavior. *Neuropsychopharmacology*, *40*(1), 238–239. https://doi.org/10.1038/npp.2014.206

Riga, D., Matos, M. R., Glas, A., Smit, A. B., Spijker, S., & Van den Oever, M. C. (2014). Optogenetic dissection of medial prefrontal cortex circuitry. *Frontiers in Systems Neuroscience*, *8*(December), 1–19. https://doi.org/10.3389/fnsys.2014.00230

Robbins, T. W. (2002). The 5-choice serial reaction time task: behavioural pharmacology and functional neurochemistry. *Psychopharmacology*, *163*, 362–380. https://doi.org/10.1007/s00213-002-1154-7

Ross, W. N. (1989). Changes in intracelluar calcium during neuron activity. *Annu. Rev. Physiol.*, (51), 491–506. Retrieved from www.annualreviews.org

Rueden, C. T., Schindelin, J., Hiner, M. C., Dezonia, B. E., Walter, A. E., Arena, E. T., & Eliceiri, K. W. (2017). ImageJ2: ImageJ for the next generation of scientific image data. *BMC Bioinformatics*, *18*, 529. https://doi.org/10.1186/s12859-017-1934-z

Seamans, J. K., Lapish, C. C., & Durstewitz, D. (2008). Comparing the prefrontal cortex of rats and primates: Insights from electrophysiology. *Neurotoxicity Research*, *14*(2–3), 249–262. https://doi.org/10.1007/BF03033814

Smith, K. S., Graybiel, A. M., Lobo, M. K., Ferguson, S., & Yang, X. W. (2014). Investigating habits: strategies, technologies and models. https://doi.org/10.3389/fnbeh.2014.00039

Totah, N. K. B., Kim, Y. B., Homayoun, H., & Moghaddam, B. (2009). Anterior cingulate neurons represent errors and preparatory attention within the same behavioral sequence. *The Journal of Neuroscience : The Official Journal of the Society for Neuroscience*, *29*(20), 6418–6426. https://doi.org/10.1523/JNEUROSCI.1142-09.2009

Turner, K. M., & Burne, T. H. J. (2014). Comprehensive Behavioural Analysis of Long Evans and Sprague-Dawley Rats Reveals Differential Effects of Housing Conditions on Tests Relevant to Neuropsychiatric Disorders. *PLoS ONE*, *9*(3), 93411. https://doi.org/10.1371/journal.pone.0093411

Uran, C., Senn, V., Yizhar, O., Hardung, S., Gibor, L., Eriksson, D., … Diester, I. (2017). A Functional Gradient in the Rodent Prefrontal Cortex Supports Behavioral Inhibition. *Current Biology*, *27*(4), 549–555. https://doi.org/10.1016/j.cub.2016.12.052

Uylings, H. B. M., & Van Eden, C. G. (1991). Chapter 3 Qualitative and quantitative comparison of the prefrontal cortex in rat and in primates, including humans. *Progress in Brain Research*, *85*(C), 31–62. https://doi.org/10.1016/S0079-6123(08)62675-8

Wang, X. (2017). *Neural circuitry mechanisms in decision-making*. Karolina Institutet, Stockholm. Retrieved from https://openarchive.ki.se/xmlui/handle/10616/45582

White, M. G., Panicker, M., Mu, C., Carter, A. M., Roberts, B. M., Dharmasri, P. A., & Mathur, B. N. (2018). Anterior Cingulate Cortex Input to the Claustrum Is Required for Top-Down Action Control. *Cell Reports*, *22*(1), 84–95. https://doi.org/10.1016/j.celrep.2017.12.023

Zalocusky, K. A., Ramakrishnan, C., Lerner, T. N., Davidson, T. J., Knutson, B., & Deisseroth, K. (2016). Nucleus accumbens D2R cells signal prior outcomes and control risky decision-making. *Nature*, *531*. https://doi.org/10.1038/nature17400

Zucker, R. S. (1999). Calcium- and activity-dependent synaptic plasticity. *Current Opinion in Neurobiology*, *9*(3), 305–313. https://doi.org/10.1016/S0959-4388(99)80045-2